University of Wollongong
Research Online

Faculty of Engineering - Papers (Archive)

Faculty of Engineering and Information Sciences

2009

Self-oriented Ca3Co4O9 thin film as an anode material for enhanced cycling stability of lithium-ion batteries

Xuebin Zhu
University of Wollongong, xuebin@uow.edu.au

Shulei Chou
University of Wollongong, shulei@uow.edu.au

Lin Wang
University of Wollongong

Qi Li
University of Wollongong, qli@uow.edu.au

Dongqi Shi
University of Wollongong, dongqi@uow.edu.au

See next page for additional authors

Follow this and additional works at: https://ro.uow.edu.au/engpapers

 Part of the Engineering Commons

https://ro.uow.edu.au/engpapers/5463

Recommended Citation

Zhu, Xuebin; Chou, Shulei; Wang, Lin; Li, Qi; Shi, Dongqi; Wang, Jiazhao; Chen, Z.; Sun, Yuping; Liu, Hua-Kun; and Dou, S. X.: Self-oriented Ca3Co4O9 thin film as an anode material for enhanced cycling stability of lithium-ion batteries 2009.
https://ro.uow.edu.au/engpapers/5463

Research Online is the open access institutional repository for the University of Wollongong. For further information contact the UOW Library: research-pubs@uow.edu.au

Authors

Xuebin Zhu, Shulei Chou, Lin Wang, Qi Li, Dongqi Shi, Jiazhao Wang, Z. Chen, Yuping Sun, Hua-Kun Liu, and S. X. Dou

This journal article is available at Research Online: https://ro.uow.edu.au/engpapers/5463

Electrochemical and Solid-State Letters, **12** (9) A176-A180 (2009)
1099-0062/2009/12(9)/A176/5/$25.00 © The Electrochemical Society

Self-Oriented $Ca_3Co_4O_9$ Thin Film as an Anode Material for Enhanced Cycling Stability of Lithium-Ion Batteries

Xue-Bin Zhu,[a,d,z] Shu-Lei Chou,[a,b,*,z] Lin Wang,[a] Qi Li,[a] Dong-Qi Shi,[a] Jia-Zhao Wang,[a,b] Zhi-Xin Chen,[c] Yu-Ping Sun,[d] Hua-Kun Liu,[a,b,] and Shi-Xue Dou[a]**

[a]*Institute for Superconducting and Electronic Materials,* [b]*Australian Research Council Centre of Excellence for Electromaterials Science, and* [c]*School of Mechanical, Materials and Mechatronic Engineering, University of Wollongong, New South Wales 2522, Australia*
[d]*Key Laboratory of Materials Physics, Institute of Solid State Physics, Chinese Academy of Sciences, Hefei 230031, People's Republic of China*

Self-oriented $Ca_3Co_4O_9$ nanoflake thin film has been prepared by a simple sol–gel method as the anode for thin-film lithium-ion batteries. The X-ray diffraction and transmission electron microscopy results show that the prepared $Ca_3Co_4O_9$/Pt film is *c*-axis self-oriented and composed of nanoflakes approximately 2 μm in diameter and 200–300 nm thick. The reversible lithium storage capacity of the $Ca_3Co_4O_9$ thin-film electrode at 1 C is around 800 mAh g^{-1}, and it retains more than 70% capacity after 50 cycles, suggesting that the $Ca_3Co_4O_9$ thin film can be used as the anode for lithium-ion batteries.
© 2009 The Electrochemical Society. [DOI: 10.1149/1.3154513] All rights reserved.

Manuscript submitted April 2, 2009; revised manuscript received May 13, 2009. Published June 18, 2009.

Rechargeable lithium-ion batteries are currently the technology of choice as power sources for portable electronic devices.[1] As one of the most important types of power supply for microsystems, thin-film lithium-ion batteries are of great interest for important applications in a variety of consumer and medical products.[2-4] The relatively low theoretical capacity of graphite anode material (372 mAh g^{-1}) has inspired intensive research to investigate alternative anode materials.[5-7] In particular, nanosized transition metal oxides have been reported to exhibit an extremely large reversible capacity.[7] However, the practical use of metal oxides has been limited by their fast capacity fading and poor cycle-life performance. Part of the problem associated with these materials has been attributed to the significant volume changes that occur during lithium intercalation and deintercalation, which may result in a loss of electrical contact and electrode failure.[8] To prevent the aggregation of the particles in electrodes, the formation of active/inactive composites has gained attention for ternary metal–oxide systems.[9-15]

Recently, Kim et al. reported that nanosized layered $Ca_3Co_4O_9$ shows a very high and reversible capacity due to the formation of Co nanoclusters embedded in a pseudoamorphous Li_2O–CaO matrix.[15] To date, $Ca_3Co_4O_9$ thin film has been prepared via the pulsed laser deposition technique[16,17] and sol–gel-based chemical solution deposition,[18] which was reported by our group. However, all the previous methods used single-crystal substrates such as Si wafer and single-crystal $LaAlO_3$, which are not suitable for lithium batteries. Moreover, there are still no reports about the usage of $Ca_3Co_4O_9$ thin film as the anode for lithium-ion batteries. In addition, a thin-film electrode without using a binder and conducting agent is very useful to investigate the mechanism of the electrochemical reaction.

In this article, we report on preparing and using self-oriented $Ca_3Co_4O_9$ thin film as the anode for thin-film lithium-ion batteries via a simple and low cost sol–gel method. The electrochemical tests show that the as-prepared $Ca_3Co_4O_9$ thin film is a very promising anode for thin-film lithium-ion batteries.

Experimental

Self-oriented $Ca_3Co_4O_9$ nanoflake thin films were prepared by a simple sol–gel method on the Pt substrate. Ca acetate (Alfa Aesar, 99.9%) and Co acetate (Alfa Aesar, 99.9%) were dissolved in propionic acid at 70°C and stirred at this temperature for 20 min; then the solution was stirred at room temperature for more than 10 h to yield a well-mixed precursor solution. The solution was then diluted with propionic acid to 1.4 M in cation concentration. Pieces of polycrystalline Pt foil were ultrasonically cleaned with acetone for 15 min before use as substrates. The films were prepared by the spin-coating method, using a rotation speed of 4000 rpm and a deposition time of 60 s. The deposited films were then baked at 300°C for 3 min on a hot plate to expel the organics. To obtain the desired thickness, the spin-coating and baking procedures were repeated six times. Finally, the baked films were annealed at 870°C for 6 h under air atmosphere.

The thin films were analyzed using an X'pert Pro MPD X-ray diffractometer (Philips, Holland) using Cu Kα radiation, a scanning electron microscope (JEOL JSM-6460A, 30 kV) equipped with energy-dispersive X-ray (EDX) spectroscopy, a field-emission scanning electron microscope (FESEM; JEOL 7500, 15 kV), and a transmission electron microscope (JEOL 2011, 200 kV). Raman spectra were recorded using a Jobin Yvon Horiba Raman spectrometer model HR800 employing a 10 mW helium/neon laser at 632.8 nm, which was filtered by a neutral density filter to reduce the laser intensity and coupled with a charge-coupled detector. The transmission electron microscopy (TEM) sample was directly peeled off from the substrate using a scalpel and loaded onto a holey carbon support film on a copper grid for TEM observations.

The electrochemical characterizations were carried out using coin cells, with the $Ca_3Co_4O_9$ thin film on the Pt substrate as the cathode and lithium foil as the counter electrode. The CR2032 coin-type cells were assembled in an argon-filled (with O_2 and H_2O levels of less than 0.1 ppm) glove box (Mbraun, Unilab, Germany). The electrolyte was 1 M $LiPF_6$ (battery grade of 99.99%, Aldrich) in a 1:2 (v/v) mixture of ethylene carbonate (anhydrous 99%, Sigma-Aldrich) and diethyl carbonate (anhydrous 99 + %, Sigma-Aldrich). The cells were galvanostatically discharged and charged in the range of 0.01–3.0 V vs Li/Li^+ at a constant current density of 643 mA g^{-1} via a Neware battery tester. The specific capacity was calculated based on the mass of $Ca_3Co_4O_9$, which was obtained from the weight difference between the plain substrate and the as-prepared sample. The typical sample weight was in the range of 0.25–0.32 mg cm^{-2}.

Results and Discussion

A typical X-ray diffraction (XRD) pattern of the $Ca_3Co_4O_9$/Pt film is shown in Fig. 1a. The derived film is (00l) oriented, although the Pt substrate is polycrystalline, which indicates that a self-oriented growth mode has been realized for the film. Usually, the orientation of a film is determined by the competition between the interface energy of the film/substrate and the surface energy of the film.[18] Because $Ca_3Co_4O_9$ has a layered structure, with the lowest

* Electrochemical Society Student Member.
** Electrochemical Society Active Member.
z E-mail: xuebin@uow.edu.au; sc478@uow.edu.au

Downloaded on 2013-07-11 to IP 203.10.91.11 address. Redistribution subject to ECS license or copyright; see ecsdl.org/site/terms_use

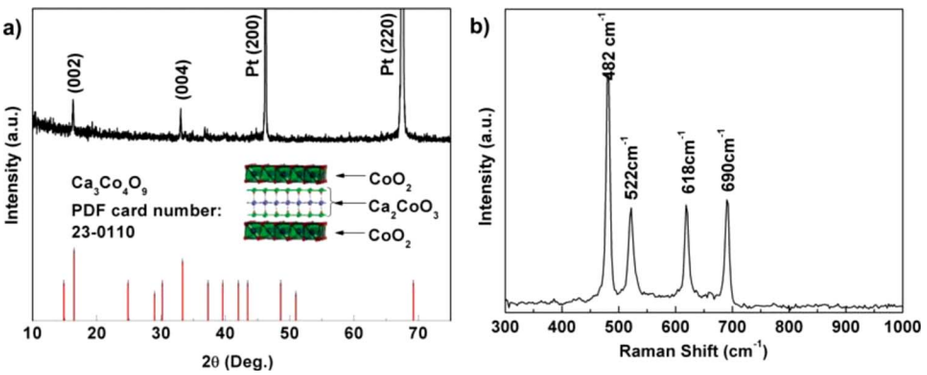

Figure 1. (Color online) (a) XRD pattern of the $Ca_3Co_4O_9$/Pt film with the inset showing the film structure and (b) Raman spectrum of the prepared film.

surface energy associated with the (00l) planes, there is preferential growth with the (00l) orientation; moreover, the crystal structures of $Ca_3Co_4O_9$ and Pt are different, meaning that the interface energy plays only a minor role in the growth orientation of the $Ca_3Co_4O_9$ film. These two factors favor the self-oriented growth mode of the $Ca_3Co_4O_9$ film with (00l) orientation, as observed from the XRD pattern.

Figure 1b shows the Raman spectrum of the prepared $Ca_3Co_4O_9$/Pt film. There are four peaks located at 482, 522, 618, and 690 cm^{-1}. Compared to the previous Raman study on the $Ca_3Co_4O_9$ single crystal,[19] these four peaks match the xx mode, although several peaks in our sample are missing, which further suggests that there is a misfit layered structure for the derived

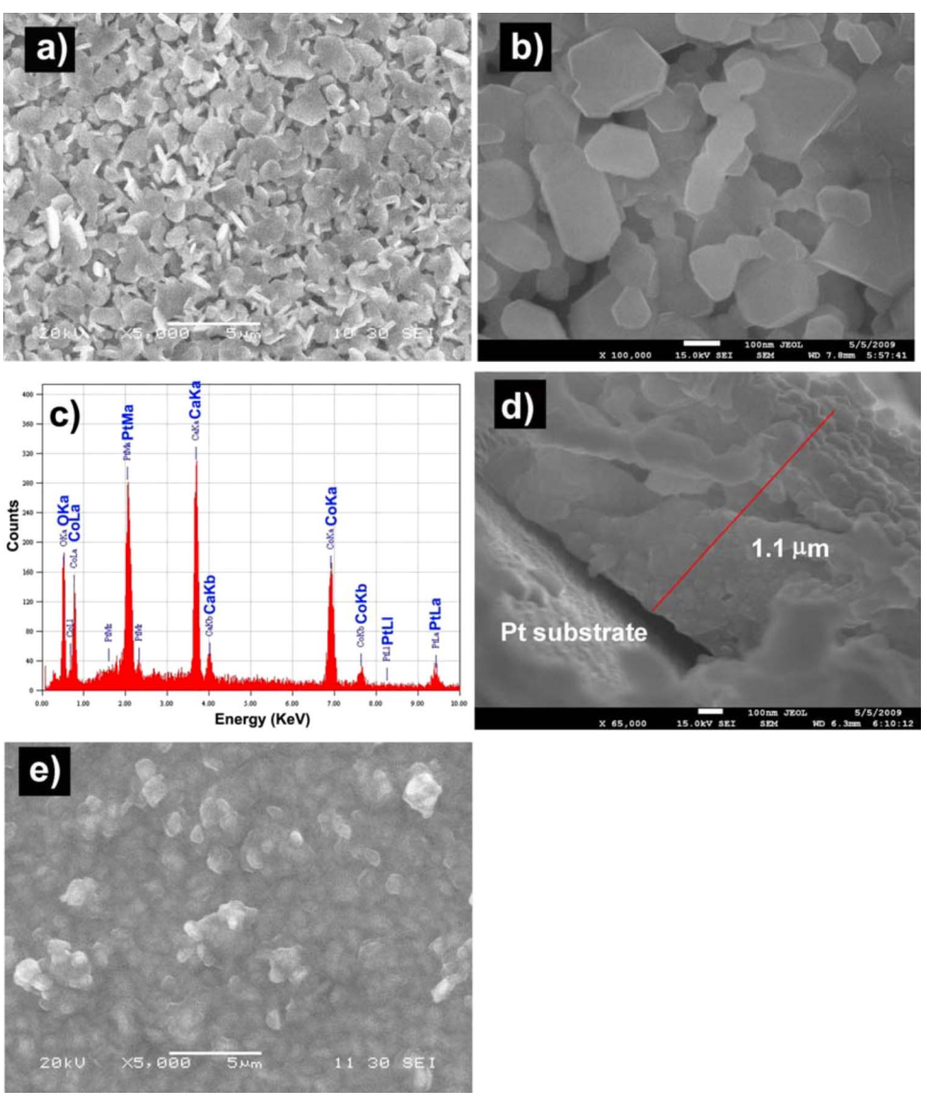

Figure 2. (Color online) (a) SEM images of the $Ca_3Co_4O_9$/Pt film before cycling and (e) after 50 cycles, (b) FESEM images of the $Ca_3Co_4O_9$/Pt film from the surface and (d) its cross-section views, and (c) EDX spectrum of the $Ca_3Co_4O_9$/Pt film.

Downloaded on 2013-07-11 to IP 203.10.91.11 address. Redistribution subject to ECS license or copyright; see ecsdl.org/site/terms_use

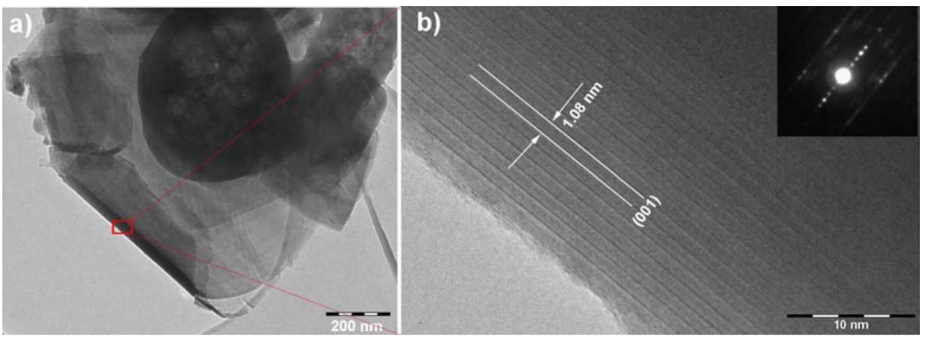

Figure 3. (Color online) (a) Typical TEM image and (b) HRTEM image of the $Ca_3Co_4O_9$ thin film with the inset of the SAED pattern.

$Ca_3Co_4O_9$ film. The peak shifting and missing peaks may be attributed to peak intensity that is negligible or masked by structural defects such as grain boundaries.

Figures 2a-d are the scanning electron microscopy (SEM) and FESEM images of the as-prepared $Ca_3Co_4O_9$/Pt film, respectively. The film is composed of nanoflakes approximately 2 μm in diameter and 200–300 nm thick. The thickness of the $Ca_3Co_4O_9$ film shown in Fig. 2d is around 1.1 μm. Combined with the XRD results, we believe the biggest facet of the nanoflakes represents the *ab* plane of the $Ca_3Co_4O_9$. That is, most of the nanoflakes have the *c*-axis orientation. Figure 2c is the EDX spectrum of the prepared $Ca_3Co_4O_9$/Pt film. The elements Ca and Co are clearly indicated, without any undesired elements, and the atomic ratio of Co:Ca is about 1.2, which is near the stoichiometry of $Ca_3Co_4O_9$, indicating that the composition of the prepared film is stoichiometric. Combined with the XRD and SEM results, it is proposed that the growth rate in the *ab*-plane direction is faster than that in the *c*-axis direction, resulting in the flakelike grains.

Further TEM observations are shown in Fig. 3. Figure 3a shows several flakelike structures of the $Ca_3Co_4O_9$ thin film with a diameter around 2 μm and a thickness around 50 nm. The thickness is smaller than in the SEM observation due to the peeling off process using a scalpel for TEM sample preparation. However, the curling edges of the flakes, which are due to the peeling off process, make it possible to investigate the cross section of the $Ca_3Co_4O_9$ flakes. The high resolution transmission electron microscopy (HRTEM) image taken from the marked area in (a) is shown in Fig. 3b, and the corresponding selected area electron diffraction (SAED) pattern for the HRTEM is shown in the inset of Fig. 3b. The diffraction spots can be assigned to the single-crystal $Ca_3Co_4O_9$ phase. The lattice fringes are visible over a large range with a spacing of 1.08 nm, which agrees with the spacing of the (001) planes of $Ca_3Co_4O_9$, indicating the good single-crystalline nature. The TEM observations confirmed that the growth of the $Ca_3Co_4O_9$ thin film is along the (001) plane, which is consistent with the XRD results showing that the $Ca_3Co_4O_9$ thin film is highly oriented along the (001) plane.

Figure 4a shows the charge–discharge curves of the $Ca_3Co_4O_9$ thin film in coin test cells using lithium as the counter and reference electrode between 0.01 and 3.0 V (vs Li^+/Li) at a current density of 1 C (C = 643 mA g^{-1}). The charge–discharge curves show similar features to those of nanosized $Ca_3Co_4O_9$ as reported in Ref. 15. The initial discharge curve can be divided into four regions, marked as I, II, III, and IV. In regions I–III, $Ca_3Co_4O_9$ reacts with lithium ions to yield a composite of CaO, Co, and Li_2O. The theoretical capacity of $Ca_3Co_4O_9$ from the reduction reaction of Co(III) to Co(0) is 643 mAh g^{-1}, corresponding to a maximum lithium uptake of 12 Li per $Ca_3Co_4O_9$. The electrode in initial discharge shows specific capacities of more than 1200 mAh g^{-1}, which is similar to what has been reported for nanosized $Ca_3Co_4O_9$. The extra capacity (re-

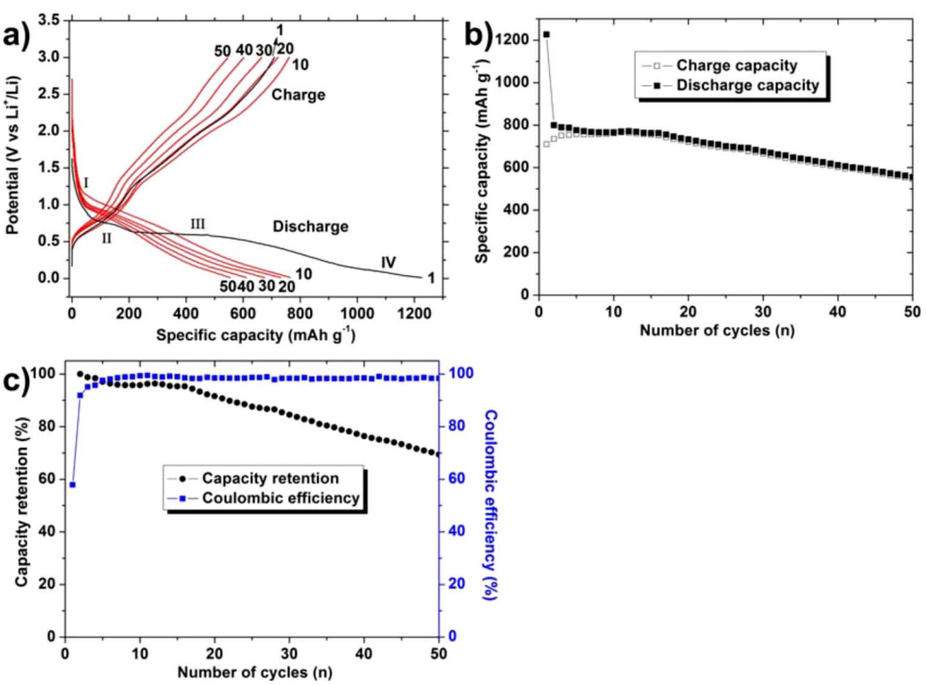

Figure 4. (Color online) (a) Charge–discharge curves, (b) cycle life, and (c) coulombic efficiency and capacity retention of the $Ca_3Co_4O_9$ thin film.

Downloaded on 2013-07-11 to IP 203.10.91.11 address. Redistribution subject to ECS license or copyright; see ecsdl.org/site/terms_use

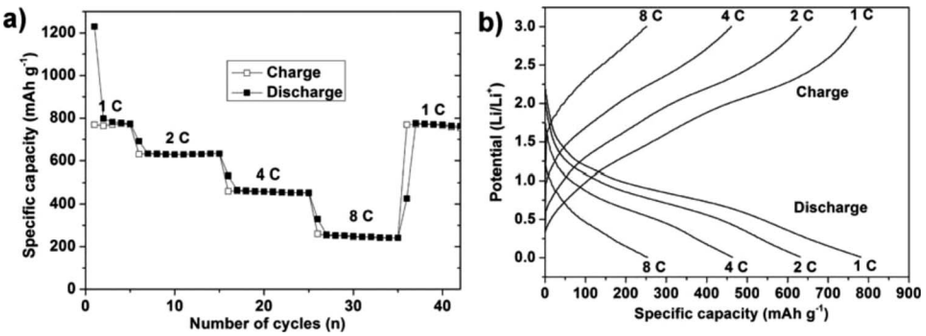

Figure 5. (a) Charge and discharge curve and (b) cycle-life curve of the $Ca_3Co_4O_9$ thin film with different current densities from 1 to 8 C.

gion IV) has been explained as the decomposition of the electrolyte to form a solid electrolyte interphase layer[20] or further lithium storage via interfacial reactions due to the charge separation at the metal/Li_2O phase boundary.[21] In region II, a small amount of lithium ions can be inserted into the layered structure of $Ca_3Co_4O_9$, which is also very common in other oxides.[20,22] The potential plateau (region II) of the $Ca_3Co_4O_9$ thin film corresponds to a capacity of around 100 mAh g^{-1}, which is much higher than for nanosized $Ca_3Co_4O_9$ powder with 50 mAh g^{-1}. The $Ca_3Co_4O_9$ thin film can take up more lithium in region II than nanosized $Ca_3Co_4O_9$. The Li-ion insertion into layered $Ca_3Co_4O_9$ is along the (001) plane. The highly oriented $Ca_3Co_4O_9$ thin film along the (001) plane can facilitate the lithium diffusion so that the Li ions can be inserted much more easily into the self-oriented $Ca_3Co_4O_9$ thin film than in randomly oriented $Ca_3Co_4O_9$ particles. The plateau for the $Ca_3Co_4O_9$ thin film in region III is around 0.6 V (vs Li^+/Li), which is much lower than for nanosized $Ca_3Co_4O_9$ around 0.9 V (vs Li^+/Li). The low potential plateau may be due to the high discharge rate used here. After the initial cycle, regions I and II of the discharge curves merge into one sloping curve. The plateau of region III increases from around 0.6 to around 0.9 V. The charge curves are all similar sloping curves. The mechanism for reversible lithium storage for $Ca_3Co_4O_9$ is summarized as follows

Initial discharge

$$12Li + Ca_3Co_4O_9 \rightarrow 3CaO + 4Co + 6Li_2O$$

After initial discharge

$$4Li_2O + 3Co \leftrightarrow Co_3O_4 + 8Li$$

The cycle stability of the $Ca_3Co_4O_9$ thin film is shown in Fig. 4b. The capacity drops slightly from the 2nd cycle to the 16th cycle, with the capacity decreasing from 800 to 750 mAh g^{-1}, and then from the 17th cycle to the 50th cycle, the capacity decreases from 750 to 550 mAh g^{-1}. The $Ca_3Co_4O_9$ thin film demonstrates a capacity as high as 550 mAh g^{-1} after 50 cycles at 1 C current density, which is better than in the previous reports on nanosized $Ca_3Co_4O_9$,[15] Co_3O_4 thin films,[23] and even Co_3O_4 nanotubes.[24] The capacity retention compared to the second cycle and the coulombic efficiency are shown in Fig. 4c. The $Ca_3Co_4O_9$ thin film can maintain approximately 70% capacity after 50 cycles compared to the second cycle, indicating the good cycling stability of the $Ca_3Co_4O_9$ thin film. The initial coulombic efficiency is 58%. The coulombic efficiency increases to 91% at the second cycle and for the following cycles is on average around 98%. The high coulombic efficiency indicates potential industrial applications of the $Ca_3Co_4O_9$ thin film.

Changing rates of current densities were also used to investigate the electrochemical performance of the $Ca_3Co_4O_9$ thin film, as shown in Fig. 5. Figure 5a shows the charge and discharge curves of the $Ca_3Co_4O_9$ thin-film electrode at different current densities. The charge and discharge curves show increasing slope with the increasing C rate. In Fig. 5b the $Ca_3Co_4O_9$ thin film shows capacities of 781, 631, 464, and 253 mAh g^{-1} at current densities of 1, 2, 4, and 8 C, respectively, indicating the relatively good high rate capability. After changing the current density back to 1 C from 8 C, the capacity of the $Ca_3Co_4O_9$ thin-film electrode was maintained compared to the fifth cycle, again showing the good capacity retention of the $Ca_3Co_4O_9$ thin-film electrode.

After cycling, the batteries were opened, and the electrodes were taken out and washed. The $Ca_3Co_4O_9$ thin film maintained good mechanical contact with the substrate during the washing. An SEM image is shown in Fig. 2e. The morphology of the cycled $Ca_3Co_4O_9$ electrode is much smoother than for the uncycled one. The nanoflakelike structure of $Ca_3Co_4O_9$ changes to one composed of nanoparticles due to the lithium intercalation and deintercalation, and the pores between different $Ca_3Co_4O_9$ nanoflakes are filled up. The good cycle stability of $Ca_3Co_4O_9$ can be explained by the buffering effect of nonreactive-nanosized CaO, which could accommodate the big volume changes in Co_3O_4.[25] With no binder or conducting agent, the high capacity retention of the $Ca_3Co_4O_9$ thin film is due to the buffering effect of CaO. Moreover, here the pores between different $Ca_3Co_4O_9$ flakes can facilitate the penetration of the electrolyte, and the self-oriented $Ca_3Co_4O_9$ structure can facilitate the lithium insertion.

Conclusion

Self-oriented $Ca_3Co_4O_9$ thin films were successfully prepared as the thin-film anode for lithium-ion batteries, using a simple sol–gel method on the polycrystalline Pt substrate. The XRD patterns and TEM observations show that the $Ca_3Co_4O_9$/Pt film is *c* axis self-oriented. SEM analysis clearly shows that the $Ca_3Co_4O_9$/Pt film is composed of nanoflakes. The capacity retention after 50 cycles is 550 mAh g^{-1}, which is much higher than that of the commercial graphite materials. These results may inspire further studies of $Ca_3Co_4O_9$ as the high capacity thin-film anode for Li-ion batteries.

Acknowledgments

The financial support provided by the Australian Research Council (ARC) through the ARC Centre of Excellence funding (no. CE0561616) is gratefully acknowledged. The authors also thank Dr. Silver for critical reading of the manuscript.

University of Wollongong assisted in meeting the publication costs of this article.

References

1. J. M. Tarascon and M. Armand, *Nature (London)*, **414**, 359 (2001).
2. J. B. Bates, G. R. Gruzalski, N. J. Dudney, C. F. Luck, and X. H. Yu, *Solid State Ionics*, **70-71**, 619 (1994).
3. J. B. Bates, N. J. Dudney, B. Neudecker, A. Ueda, and C. D. Evans, *Solid State Ionics*, **135**, 33 (2000).
4. G. J. La O', H. J. In, E. Crumlin, G. Barbastathis, and Y. Shao-Horn, *Int. J. Energy Res.*, **31**, 548 (2007).
5. A. S. Arico, P. Bruce, B. Scrosati, J. M. Tarascon, and W. Van Schalkwijk, *Nature Mater.*, **4**, 366 (2005).
6. Y. Idota, T. Kubota, A. Matsufuji, Y. Maekawa, and T. Miyasaka, *Science*, **276**, 1395 (1997).
7. P. Poizot, S. Laruelle, S. Grugeon, L. Dupont, and J. M. Tarascon, *Nature (London)*, **407**, 496 (2000).
8. D. Larcher, S. Beattie, M. Morcrette, K. Edstroem, J. C. Jumas, and J. M. Tarascon,

Downloaded on 2013-07-11 to IP 203.10.91.11 address. Redistribution subject to ECS license or copyright; see ecsdl.org/site/terms_use

J. Mater. Chem., **17**, 3759 (2007).
9. J. Read, D. Foster, J. Wolfenstine, and W. Behl, *J. Power Sources*, **96**, 277 (2001).
10. T. P. Kumar, R. Ramesh, Y. Y. Lin, and G. T. K. Fey, *Electrochem. Commun.*, **6**, 520 (2004).
11. S. A. Needham, G. X. Wang, K. Konstantinov, Y. Tournayre, Z. Lao, and H. K. Liu, *Electrochem. Solid-State Lett.*, **9**, A315 (2006).
12. X. H. Huang, J. P. Tu, C. Q. Zhang, and J. Y. Xiang, *Electrochem. Commun.*, **9**, 1180 (2007).
13. R. Yang, Z. Wang, J. Liu, and L. Chen, *Electrochem. Solid-State Lett.*, **7**, A496 (2004).
14. O. Mao, R. L. Turner, I. A. Courtney, B. D. Fredericksen, M. I. Buckett, L. J. Krause, and J. R. Dahn, *Electrochem. Solid-State Lett.*, **2**, 3 (1999).
15. D. W. Kim, Y. D. Ko, J. G. Park, and B. K. Kim, *Angew. Chem., Int. Ed.*, **46**, 6654 (2007).
16. H. W. Eng, W. Prellier, S. Herbert, D. Grebille, L. Michin, and B. Mercey, *J. Appl. Phys.*, **97**, 013706 (2005).
17. A. Pautrat, H. W. Eng, and W. Prellier, *Phys. Rev. B*, **72**, 233405 (2005).
18. X. B. Zhu, Y. P. Sun, H. C. Lei, X. H. Li, R. Ang, B. C. Zhao, W. H. Song, D. Q. Shi, and S. X. Dou, *J. Appl. Phys.*, **102**, 103519 (2007).
19. M. An, S. K. Yuan, Y. Wu, Q. M. Zhang, X. G. Luo, and X. H. Chen, *Phys. Rev. B*, **76**, 024305 (2007).
20. D. Larcher, C. Masquelier, D. Bonnin, Y. Chabre, V. Masson, J. B. Leriche, and J. M. Tarascon, *J. Electrochem. Soc.*, **150**, A133 (2003).
21. J. Jamnik and J. Maier, *Phys. Chem. Chem. Phys.*, **5**, 5215 (2003).
22. X. L. Wu, Y. G. Guo, L. J. Wan, and C. W. Hu, *J. Phys. Chem. C*, **112**, 16824 (2008).
23. S. L. Chou, J. Z. Wang, H. K. Liu, and S. X. Dou, *J. Power Sources*, **182**, 359 (2008).
24. W. Y. Li, L. N. Xu, and J. Chen, *Adv. Funct. Mater.*, **15**, 851 (2005).
25. H. J. Liu, S. H. Bo, W. J. Cui, F. Li, C. X. Wang, and Y. Y. Xia, *Electrochim. Acta*, **53**, 6497 (2008).

Downloaded on 2013-07-11 to IP 203.10.91.11 address. Redistribution subject to ECS license or copyright; see ecsdl.org/site/terms_use